

THE INFRARED LIGHT CURVE OF SN 2011FE IN M101 AND THE DISTANCE TO M101

T. MATHESON¹, R. R. JOYCE¹, L. E. ALLEN¹, A. SAHA¹, D. R. SILVA¹, W. M. WOOD-VASEY², J. J. ADAMS³, R. E. ANDERSON⁴, T. L. BECK⁴, M. C. BENTZ⁵, M. A. BERSHADY⁶, W. S. BINKERT¹, K. BUTLER¹, M. A. CAMARATA⁷, A. EIGENBROT⁶, M. EVERETT¹, J. S. GALLAGHER⁶, P. M. GARNAVICH⁸, E. GLIKMAN⁹, D. HARBECK¹⁰, J. R. HARGIS¹¹, H. HERBST⁶, E. P. HORCH⁷, S. B. HOWELL¹², S. JHA¹³, J. F. KACZMAREK⁶, P. KNEZEK^{10,1}, E. MANNE-NICHOLAS⁵, R. D. MATHIEU⁶, M. MEIXNER⁴, K. MILLIMAN⁶, J. POWER¹, J. RAJAGOPAL¹, K. REETZ¹, K. L. RHODE¹¹, A. SCHECHTMAN-ROOK⁶, M. E. SCHWAMB⁹, H. SCHWEIKER¹⁰, B. SIMMONS⁹, J. D. SIMON³, D. SUMMERS¹, M. D. YOUNG¹¹, A. WEYANT², E. M. WILCOTS⁶, G. WILL¹, D. WILLIAMS¹

ABSTRACT

We present near infra-red light curves of supernova (SN) 2011fe in M101, including 34 epochs in *H* band starting fourteen days before maximum brightness in the *B*-band. The light curve data were obtained with the WIYN High-Resolution Infrared Camera (WHIRC). When the data are calibrated using templates of other Type Ia SNe, we derive an apparent *H*-band magnitude at the epoch of *B*-band maximum of 10.85 ± 0.04 . This implies a distance modulus for M101 that ranges from 28.86 to 29.17 mag, depending on which absolute calibration for Type Ia SNe is used.

Subject headings: galaxies: distances and redshifts — galaxies: individual (M101) — supernovae: individual (SN 2011fe)

1. INTRODUCTION

Supernova 2011fe was discovered soon after explosion in the nearby galaxy M101 (NGC 5457) by the Palomar Transient Factory (Rau et al. 2009; Law et al. 2009) on 2011 August 24.167 UT (all calendar dates herein are UT) and rapidly classified as a supernova of Type Ia (SN Ia) (Nugent et al. 2011a,b, identified initially as PTF11kly). This was the brightest SN Ia since SN 1972E in NGC 5253 (see, e.g., Kirshner et al. 1973), although SN 1986G remains the nearest SN Ia (e.g., Phillips et al. 1987). The combination of proximity, early discovery, and modern observing resources makes this SN a rare gift that can be studied in unprecedented detail.

Over the last two decades, the reliability of SNe Ia as calibratable standard candles has been securely established. Specifically, the regression of peak bright-

ness in optical magnitudes (corrected for reddening and *a priori* second parameter effects, usually light-curve shape) against recession velocity v_r (the Hubble diagram) in the range $1200 \text{ km s}^{-1} \leq v_r \leq 30,000 \text{ km s}^{-1}$ has been shown to be almost linear and to have a scatter of only 0.13 mag rms (e.g., Hamuy et al. 1996; Riess et al. 1996; Parodi et al. 2000; Guy et al. 2005; Jha et al. 2007; Conley et al. 2008; Hicken et al. 2009; Kessler et al. 2009; Folatelli et al. 2010; Burns et al. 2011; Mandel et al. 2009, 2011). SNe Ia are thus largely free of any Malmquist bias, and by virtue of their brightness, are cosmological probes at distances where peculiar motions of galaxies are insignificant compared to the expansion velocity of the cosmic manifold. Their consequent use as probes of cosmic acceleration is now well known (e.g., Riess et al. 1998; Perlmutter et al. 1999; Astier et al. 2006; Wood-Vasey et al. 2007; Sullivan et al. 2011).

Photometry of SNe Ia in the near infra-red (NIR) has shown even greater promise for use as a standard candle (for a recent review of the NIR properties of SNe Ia, see Phillips (2011)). The effects of extinction are greatly reduced and they appear to have relatively constant peak magnitudes in *J*, *H*, and *K_s* (Meikle 2000; Krisciunas et al. 2004a,b, 2007). The scatter in the NIR Hubble diagram is ~ 0.15 mag *without* the light-curve shape corrections necessary for optical bands (Krisciunas et al. 2004a; Wood-Vasey et al. 2008; Folatelli et al. 2010). Motivated by this, we began a Director's discretionary time program to observe SN 2011fe with the WIYN High-Resolution Infrared Camera (WHIRC) NIR camera at the WIYN 3.5-m telescope¹⁴ on Kitt Peak, taking advantage of the instrumentation deployment that allows for the use of the NIR camera even when other instruments are scheduled for a given night.

matheson@noao.edu

¹ National Optical Astronomy Observatory, 950 N. Cherry Avenue, Tucson, AZ 85719

² Pittsburgh Particle Physics, Astrophysics, and Cosmology Center (PITT-PACC), University of Pittsburgh, 3941 O'Hara Street, Pittsburgh, PA 15260, USA

³ Observatories of the Carnegie Institution of Washington, 813 Santa Barbara Street, Pasadena, CA 91101, USA

⁴ Space Telescope Science Institute, 3700 San Martin Drive, Baltimore, MD 21218 USA

⁵ Department of Physics and Astronomy, Georgia State University, Astronomy Offices, One Park Place South SE, Suite 700, Atlanta, GA 30303, USA

⁶ Department of Astronomy, University of Wisconsin-Madison, 475 N. Charter Street, Madison, WI 53706, USA

⁷ Department of Physics, Southern Connecticut State University, 501 Crescent Street, New Haven, CT 06515, USA

⁸ Department of Physics, University of Notre Dame, Notre Dame, IN 46556, USA

⁹ Department of Astronomy, Yale University, New Haven, CT 06511, USA

¹⁰ WIYN Observatory, 950 N. Cherry Avenue, Tucson, AZ 85719 USA

¹¹ Department of Astronomy, Indiana University, Bloomington, IN 47405, USA

¹² NASA Ames Research Center, Moffett Field, CA 94035

¹³ Department of Physics and Astronomy, Rutgers, The State University of New Jersey, Piscataway, NJ 08854-8019, USA

¹⁴ The WIYN Observatory is a joint facility of the University of Wisconsin, Indiana University, Yale University, and the National Optical Astronomy Observatory.

2. OBSERVATIONS AND DATA REDUCTION

We imaged the SN on 34 nights between 2011 Aug 27 and 2011 Oct 26 with WHIRC. The WHIRC camera (Meixner et al. 2010) contains a 2048² HgCdTe array with a field of view of 3'3" x 3'3" and a pixel scale of $\sim 0.1''$ per pixel. We obtained observations in the H band during each visit and observations in the J and K_s bands for most of the visits (see Table 1 for details). On photometric nights, a standard star at similar air mass (P133C, Persson et al. 1998) was observed in the same filters. A typical observing sequence consisted of 20 to 30 second exposures in a 5-point cross-shaped dither pattern with $\sim 20''$ dithers. Most nights, this sequence was executed twice in the H band, with a $5''$ random offset of the telescope between maps.

Data were reduced in IRAF¹⁵ as prescribed in the WHIRC Reduction Manual (Joyce 2009). The raw images were corrected for non-linearity and sky subtracted using a median-filtered sky frame obtained from each 5-point map. The images were flat-fielded with dome flats corrected for the pupil ghost (an inherent feature of WHIRC images resulting from internal reflections from the optical elements) using the IRAF routine `mscred.rmpupil`. Aperture photometry was performed on each sky-subtracted, flatfielded image using typical apertures of $3''$ diameter and a surrounding sky annulus of $0.5''$ width. On nights where the seeing FWHM was greater than $1.0''$, a 4 or $5''$ aperture diameter was used. We did not have a template image to subtract the host galaxy light as is commonly done for SNe. The host background is relatively smooth in the region chosen for the sky. In addition, inspection of Two Micron All Sky Survey (2MASS; Skrutskie et al. 2006) images of the region reveal no point source at the location of SN 2011fe to 3σ limits of 17.5, 17.4, and 16.7 in J , H , and K_s , respectively, well below the brightness of the SN itself.

All photometry of SN 2011fe was calibrated relative to a local calibrator, the nearby 2MASS source 14031367+5415431. This star lies approximately $80''$ SW of SN 2011fe, within the same WHIRC field, so the relative photometry should be independent of atmospheric transparency or extinction. Because of the relatively large (0.024 mag) published uncertainties in the 2MASS calibration, the nearby photometric standard P133C (Persson et al. 1998) was observed on ten photometric nights to calibrate the local 2MASS standard using canonical atmospheric extinction coefficients of 0.08, 0.04, and 0.07 mag/airmass for the J , H , and K_s filters, respectively. The corrections to the 2MASS magnitudes of the local calibrator to the Persson standard were small (~ 0.01 mag), with our final values being 12.008 ± 0.009 mag, 11.471 ± 0.008 mag, and 11.405 ± 0.011 mag in J , H , and K_s , respectively. The flux-calibrated magnitudes of SN 2011fe are presented in Table 1 and plotted in Figure 1. The quoted uncertainties are the rms of the mean of the individual images with the error in the calibration of the standard (which is the dominant source of error) included.

In addition, the brightness of the local standard

2MASS 14031367+5415431 was measured relative to another 2MASS star in the field (14025941+5416266) on all nights to ensure against intrinsic variability of the local standard. Over the course of the observations, the rms uncertainty in the differential photometry of these two stars was 0.015 mag, which can be considered an upper limit on any intrinsic variability. If nights judged not to be photometric are excluded, this rms uncertainty decreases to 0.010 mag.

3. ANALYSIS

In order to calibrate SN 2011fe against other SNe Ia, we compared our photometry with that of Wood-Vasey et al. (2008). Kattner et al. (2012) have shown that there is a weak relationship between absolute luminosity and decline rate in the J and H bands. Optical photometry of SN 2011fe indicates that it is a “normal” SN Ia with a $\Delta m_{15}(B)$ value of ~ 1.2 (Richmond & Smith 2012), so we will not make any corrections for decline rate (as the correction suggested by Kattner et al. (2012) is minimal at this decline rate). Wood-Vasey et al. (2008) provide templates of light curves of SNe Ia in J , H , and K_s . We fit our data to the templates using a χ^2 minimization. We restricted the fit to epochs ranging from 10 days before B -band maximum light (the earliest points in the templates) to 25 days after B -band maximum (when differences in filter bandpasses and spectral features combine to create deviations from the templates). We restricted the fit to 19 days after B -band maximum for the J band as it showed larger deviations from the templates. The J filter in WHIRC is significantly different than the J filter used for the Wood-Vasey et al. (2008) templates (and the K_s filter has differences as well). Details on the WHIRC filter bandpasses are available from the WHIRC website¹⁶ and are shown compared to 2MASS and Carnegie Supernova Program (CSP; Contreras et al. 2010) filter bandpasses in Figure 2.

The Wood-Vasey et al. (2008) templates are defined relative to B -band maximum. We did not have optical photometry, so both the scaling in magnitude and the epoch were free parameters in the fit. For all three bandpasses, we derived the same epoch of B -band maximum, 2011 September 9.9 ± 0.2 (MJD 55813.9, consistent with the time derived by other groups; W. Li, private communication).

From the Wood-Vasey et al. (2008) templates we can derive the maximum in each passband (we missed a measurement of that epoch as a result of poor weather) as well as the magnitude in each band at the time of B -band maximum. The values at B -band maximum are the fiducial points of the Wood-Vasey et al. (2008) templates. For the maximum in each bandpass, we find $J_{\max} = 10.51 \pm 0.04$ mag, $H_{\max} = 10.75 \pm 0.04$ mag, and $K_{s\max} = 10.64 \pm 0.05$ mag. At B -band maximum, we find $J_{B\max} = 10.62 \pm 0.04$ mag, $H_{B\max} = 10.85 \pm 0.04$ mag, and $K_{sB\max} = 10.68 \pm 0.05$ mag. To evaluate the uncertainty for each value, we used the Wood-Vasey et al. (2008) light curves that had at least three points within three days of B -band maximum to calculate the error of the mean for the template in each band. Templates derived from data taken by the CSP (Contreras et al. 2010)

¹⁵ IRAF is distributed by the National Optical Astronomy Observatory, which is operated by the Association of Universities for Research in Astronomy, Inc., under cooperative agreement with the National Science Foundation.

¹⁶ <http://www.noao.edu/kpno/manuals/whirc/filters.html>

as well as the Wood-Vasey et al. (2008) data (Shappee & Jha, in prep.) show essentially the same structure near maximum brightness where we are performing the fit and result in similar fits.

Krisciunas et al. (2004b) present a third-order polynomial fit for their NIR light curves of SNe Ia. This curve is not a good match for our points over the nominal range given by Krisciunas et al. (2004b), most likely as result of their dataset having few points before maximum. If we restrict the fit to just the points near maximum, we derive $J_{\max} = 10.49 \pm 0.06$ mag, $H_{\max} = 10.76 \pm 0.08$ mag, and $K_{s\max} = 10.65 \pm 0.08$ mag (uncertainties are dominated by the rms values from Krisciunas et al. (2004b) fits). All derived magnitudes are consistent with those found using the Wood-Vasey et al. (2008) templates.

We have not applied any K corrections to our photometry. The redshift of M101 is 0.000804 ± 0.000007 (de Vaucouleurs et al. 1991), so any K correction will be minimal. The Schlegel et al. (1998) dust maps imply a foreground extinction of $A_V = 0.028$ mag, and thus values in the J , H , and K_s bands less than 0.01 mag. Based on narrow Na I D absorption lines in the spectra of SN 2011fe, Nugent et al. (2011b) derive a host-galaxy extinction of $A_V = 0.04$ mag (Patat et al. (2011) report a similar result). Again, this implies extinctions in the H and K_s bands less than 0.01 mag, while the extinction in the J band is ~ 0.01 mag. Given these minimal values, we do not apply any correction to our photometry.

4. DISCUSSION

To establish the absolute luminosity calibration of SNe Ia, we need SNe in nearby galaxies to which distances can be determined by other methods. There is a rich history of obtaining Cepheid-based distances to such host galaxies, using the *HST* (e.g., Sandage et al. 2006; Gibson et al. 2000; Freedman et al. 2001; Riess et al. 2009). A discussion of the details associated with these techniques is beyond the scope of this paper. Rather, we recognize that M101 provides a better platform for the absolute magnitude calibration, because it is nearby and its distance is better determinable, if not already determined. In addition, the demonstration by Krisciunas et al. (2004a,b); Wood-Vasey et al. (2008) that the H -band light curves and peak brightnesses of SNe Ia are independent of second parameter characteristics of individual SNe (in addition, of course to being almost unaffected by reddening), provides a method that mitigates many of the issues that have plagued the earlier attempts and resulted in controversy. The weak relationship between luminosity and decline-rate in the J and H bands found by Kattner et al. (2012) does add some potential complications for SNe Ia in the infra-red in general, but not for the particular case of SN 2011fe as its $\Delta m_{15}(B)$ value of 1.2 (Richmond & Smith 2012). Here we use our data for SN 2011fe to discuss the absolute magnitude anchor for the H -band calibration of SNe Ia, by comparing against currently available Cepheid distances to M101.

For the purpose of comparing our data to absolute calibrations of SNe Ia in the infra-red, we will focus on the H band, although similar results can be found using the J and K_s bands. As can be seen in Figure 2, the H filter bandpass is the most similar across the data sets used for absolute calibration (PAIRITEL and CSP) as well

as the WHIRC data. In addition, not all derivations of absolute calibrations include the K_s band. As an example, Wood-Vasey et al. (2008) use H -band magnitudes at B_{\max} and the Hubble diagram (recession velocity vs apparent magnitude) to, in effect, derive that the absolute H -band magnitude at B_{\max} is:

$$M(H_{B_{\max}}) - 5\log(H_0/72) = -18.08 \pm 0.15 \quad (1)$$

They then quote $M(H_{B_{\max}}) = -18.08 \pm 0.15$ mag, by adopting $H_0 = 72 \text{ km s}^{-1} \text{ Mpc}^{-1}$ ¹⁷. Our measured value of $H_{B_{\max}} = 10.85 \pm 0.04$ mag for SN 2011fe yields a distance modulus $(m - M)_0 = 28.93 \pm 0.16$ mag if H_0 is indeed $72 \text{ km s}^{-1} \text{ Mpc}^{-1}$. More precisely, SN 2011fe gives the distance modulus to M101 as:

$$(m - M) + 5\log(H_0/72) = 28.93 \pm 0.16 \text{ mag} \quad (2)$$

Note that the main uncertainty comes from the intrinsic rms of 0.15 mag in H -band absolute calibration as reported by Wood-Vasey et al. (2008), and not from the relatively insignificant uncertainty in the determination of the H magnitude at the epoch of B_{\max} . Table 2 lists the various absolute infra-red calibrations for SNe Ia (all essentially based on a cosmology that assumes $H_0 = 72 \text{ km s}^{-1} \text{ Mpc}^{-1}$) and the distance moduli to M101 derived from these calibrations using our apparent magnitudes for SN 2011fe. Again, in each case the uncertainty is dominated by the absolute calibration, not the photometry of SN 2011fe. There is a wide range in the absolute calibrations, yielding a span of 0.31 mag in distance modulus depending on the specific calibration used. The source of this dispersion is not clear, but may be the result of different filters, corrections to those filters, and assumptions that went into the individual analyses. Note also that these calibrations are not all independent, as many use the same data sets and analysis tools. Until the infra-red absolute magnitudes of SNe Ia are more firmly settled, there will be some question about their cosmological utility.

Freedman et al. (2001) concluded that the distance modulus to M101 from Cepheids is 29.13 ± 0.11 mag, where the Cepheid distance scale zero-point rests on an adopted LMC distance modulus (μ_0) of 18.50 mag. Saha et al. (2006) give 29.17 ± 0.09 mag from an alternative analysis of the same data and an adopted $\mu_0(LMC)$ of 18.54 mag. A more recent comprehensive and completely independent study of Cepheids in M101 yields 29.04 ± 0.19 mag (Shappee & Stanek 2011), where the Cepheid scale is based on the maser distance to NGC 4258, which is tantamount to $\mu_0(LMC) = 18.41$ mag. The differences among these three results thus rest entirely on the adopted zero-point for the respective Cepheid P-L relations used by the three sets of authors. Comparing the conditional ($H_0 = 72$) H -band distance moduli to M101 from Table 2 to the Cepheid distances and using equation 2 (with the appropriate infra-red calibration), one finds the infra-red distances can accommodate H_0 values from 64 to $74 \text{ km s}^{-1} \text{ Mpc}^{-1}$. Using H -band photometry with NICMOS on *HST*, and an assumed LMC modulus of 18.50 mag, Macri et al. (2001) obtained distance moduli of 29.53 and 29.19 mag from

¹⁷ Using only the PAIRITEL subsample of Wood-Vasey et al. (2008) to facilitate cross-comparisons with independent samples.

Cepheids (relative to LMC Cepheids, without any metallicity dependence modeling) in outer and inner fields of M101, respectively. They concluded that in addition to metallicity differences, photometry errors from blending are a likely contributor to the observed difference (with the inner field distance erring on the side of appearing too close).

In addition, there are published distances to M101 using non-Cepheid based methods. Tip of the red giant branch (TRGB) results span the gamut from $(m-M)_0 = 29.05 \pm 0.14$ mag (Shappee & Stanek 2011) to 29.34 ± 0.09 mag (Rizzi et al. 2007) and 29.42 ± 0.11 mag (Sakai et al. 2004). Tammann & Reindl (2011) adopt the mean of the last 2 values when deriving H_0 from the visible light curve of SN 2011fe. Using the planetary nebulae luminosity function method Feldmeier et al. (1996) obtained $(m-M)_0 = 29.42 \pm 0.15$ mag. Figure 3 graphically demonstrates the distance estimates for M101 discussed herein (using the H -band calibration for SN 2011fe). Presented with this range of results, and given the state of the art uncertainties in our understanding of metallicity dependence and its inter-relation with de-reddening procedures there is no compelling argument that can pinpoint the determined distance to M101 better than the likely range from 29.04 to 29.42 mag. For this range of possible moduli and the range of conditional moduli implied by the H -band magnitude of SN 2011fe, values of H_0 from 56 to 76 km s⁻¹ Mpc⁻¹ cannot be ruled out from this SN alone.

It is sobering that M101, which is nearer than any of the SNe Ia calibrating host galaxies used by Freedman et al. (2001) or Riess et al. (2011), and for which there are multiple independent distance determinations, has resulting distance moduli that span a range

of ~ 0.4 mag. Other calibrator host-galaxies at distances comparable to Virgo and beyond do not offer such cross-validation to scrutinize the robustness of their derived distances. The source of uncertainty in the distance moduli derived from the magnitudes of SN 2011fe is not just the measurement or the calibration of the SNe Ia. It is also necessary to resolve the Cepheid and TRGB distance scales and their systematics before a better than 5% accuracy for H_0 can be asserted.

5. CONCLUSIONS

We have presented J , H , and K_s light curves of SN 2011fe in M101. The light curves appear to be those of a normal SN Ia. Our apparent magnitude in the H band at the epoch of B -band maximum is 10.85 ± 0.04 , implying distance moduli to M101 based on various infrared absolute calibrations that span a range from 28.86 to 29.17 mag. This dispersion is comparable to that for traditional distance measures to M101 (29.04 to 29.42 mag). This is, however, only one object in a class that still exhibits a small, but significant, intrinsic spread in peak magnitudes. From the dispersion in absolute calibrations of SNe Ia in the infra-red, it is clear that they are not yet fully understood.

We would like to thank the referee, Mark Phillips, for extremely useful comments and suggestions. We would also like to thank the WIYN Observatory for their support of this program. T.M. acknowledges many useful conversations with Chris Burns on the nature of SN light curves in the infra-red. T.M. dedicates this paper to the memory of his friend and colleague, Dr. Weidong Li.

Facilities: WIYN

REFERENCES

- Astier, P., Guy, J., Regnault, N., et al. 2006, *A&A*, 447, 31
 Burns, C. R., Stritzinger, M., Phillips, M. M., et al. 2011, *AJ*, 141, 19
 Conley, A., Sullivan, M., Hsiao, E. Y., et al. 2008, *ApJ*, 681, 482
 Contreras, C., Hamuy, M., Phillips, M. M., et al. 2010, *AJ*, 139, 519
 de Vaucouleurs, G., de Vaucouleurs, A., Corwin, H. G., Jr., et al. 1991, Volume 1-3, XII, 2069 pp. 7 figs.. Springer-Verlag Berlin Heidelberg New York
 Feldmeier, J. J., Ciardullo, R., & Jacoby, G. H. 1996, *ApJ*, 461, L25
 Folatelli, G., Phillips, M. M., Burns, C. R., et al. 2010, *AJ*, 139, 120
 Freedman, W. L., Madore, B. F., Gibson, B. K., et al. 2001, *ApJ*, 553, 47
 Gibson, B. K., Stetson, P. B., Freedman, W. L., et al. 2000, *ApJ*, 529, 723
 Guy, J., Astier, P., Nobili, S., Regnault, N., & Pain, R. 2005, *A&A*, 443, 781
 Hamuy, M., Phillips, M. M., Suntzeff, N. B., et al. 1996, *AJ*, 112, 2398
 Hicken, M., Challis, P., Jha, S., et al. 2009, *ApJ*, 700, 331
 Jha, S., Riess, A. G., & Kirshner, R. P. 2007, *ApJ*, 659, 122
 Joyce, D., 2009, WIYN High-Resolution Infrared Camera (WHIRC) Quick Guide to Data Reduction Version 1.03 (Tucson, AZ: NOAO), http://www.noao.edu/kpno/manuals/whirc/WHIRC_Datared_090824.pdf
 Kattner, S., Leonard, D. C., Burns, C. R., et al. 2012, *PASP*, 124, 114
 Kessler, R., Becker, A. C., Cinabro, D., et al. 2009, *ApJS*, 185, 32
 Kirshner, R. P., Willner, S. P., Becklin, E. E., Neugebauer, G., & Oke, J. B., 1973, *ApJ*, 180, 97
 Krisciunas, K., Garnavich, P. M., Stanishev, V., et al. 2007, *AJ*, 133, 58
 Krisciunas, K., Phillips, M. M., & Suntzeff, N. B. 2004a, *ApJ*, 602, L81
 Krisciunas, K., Suntzeff, N. B., Phillips, M. M., et al. 2004b, *AJ*, 128, 3034
 Law, N. M., Kulkarni, S. R., Dekany, R. G., et al. 2009, *PASP*, 121, 1395
 Macri, L. M., Calzetti, D., Freedman, W. L., et al. 2001, *ApJ*, 549, 71
 Mandel, K. S., Narayan, G., & Kirshner, R. P. 2011, *ApJ*, 731, 120
 Mandel, K. S., Wood-Vasey, W. M., Friedman, A. S., & Kirshner, R. P. 2009, *ApJ*, 704, 629
 Meikle, W. P. S. 2000, *MNRAS*, 314, 782
 Meixner, M., Smee, S., Doering, R. L., et al. 2010, *PASP*, 122, 451
 Nugent, P., Sullivan, M., Bersier, D., et al. 2011a, *The Astronomer's Telegram*, 3581, 1
 Nugent, P. E., Sullivan, M., Cenko, S. B., et al. 2011b, *Nature*, 480, 344
 Parodi, B. R., Saha, A., Sandage, A., & Tammann, G. A. 2000, *ApJ*, 540, 634
 Patat, F., Cordiner, M. A., Cox, N. L. J., et al. 2011, *arXiv:1112.0247*
 Perlmutter, S., Aldering, G., Goldhaber, G., et al. 1999, *ApJ*, 517, 565
 Perlmutter, S. E., Murphy, D. C., Krzeminski, W., Roth, M., & Rieke, M. J. 1998, *AJ*, 116, 2475
 Phillips, M. M. 2011, *PASA*, in press, *arXiv:1111.4463*
 Phillips, M. M., Phillips, A. C., Heathcote, S. R., et al. 1987, *PASP*, 99, 592
 Rau, A., Kulkarni, S. R., Law, N. M., et al. 2009, *PASP*, 121, 1334
 Richmond, M. W., & Smith, H. A. 2012, *arXiv:1203.4013*

- Riess, A. G., Filippenko, A. V., Challis, P., et al. 1998, *AJ*, 116, 1009
- Riess, A. G., Macri, L., Li, W., et al. 2009, *ApJS*, 183, 109
- Riess, A. G., Press, W. H., & Kirshner, R. P. 1996, *ApJ*, 473, 88
- Riess, A. G., Macri, L., Casertano, S., et al. 2011, *ApJ*, 730, 119
- Rizzi, L., Tully, R. B., Makarov, D., et al. 2007, *ApJ*, 661, 815
- Saha, A., Thim, F., Tammann, G. A., Reindl, B., & Sandage, A. 2006, *ApJS*, 165, 108
- Sakai, S., Ferrarese, L., Kennicutt, R. C., Jr., & Saha, A. 2004 *ApJ* 608, 42
- Sandage, A., Tammann, G. A., Saha, A., et al. 2006, *ApJ*, 653, 843
- Schlegel, D. J., Finkbeiner, D. P., & Davis, M. 1998, *ApJ*, 500, 525
- Shappee, B. J., & Stanek, K. Z. 2011, *ApJ*, 733, 124
- Skrutskie, M. F., Cutri, R. M., Stiening, R., et al. 2006, *AJ*, 131, 1163
- Sullivan, M., Guy, J., Conley, A., et al. 2011, *ApJ*, 737, 102
- Tammann, G. A., & Reindl, B. 2011, arXiv:1112.0439
- Wood-Vasey, W. M., Friedman, A. S., Bloom, J. S., et al. 2008, *ApJ*, 689, 377
- Wood-Vasey, W. M., Miknaitis, G., Stubbs, C. W., et al. 2007, *ApJ*, 666, 694

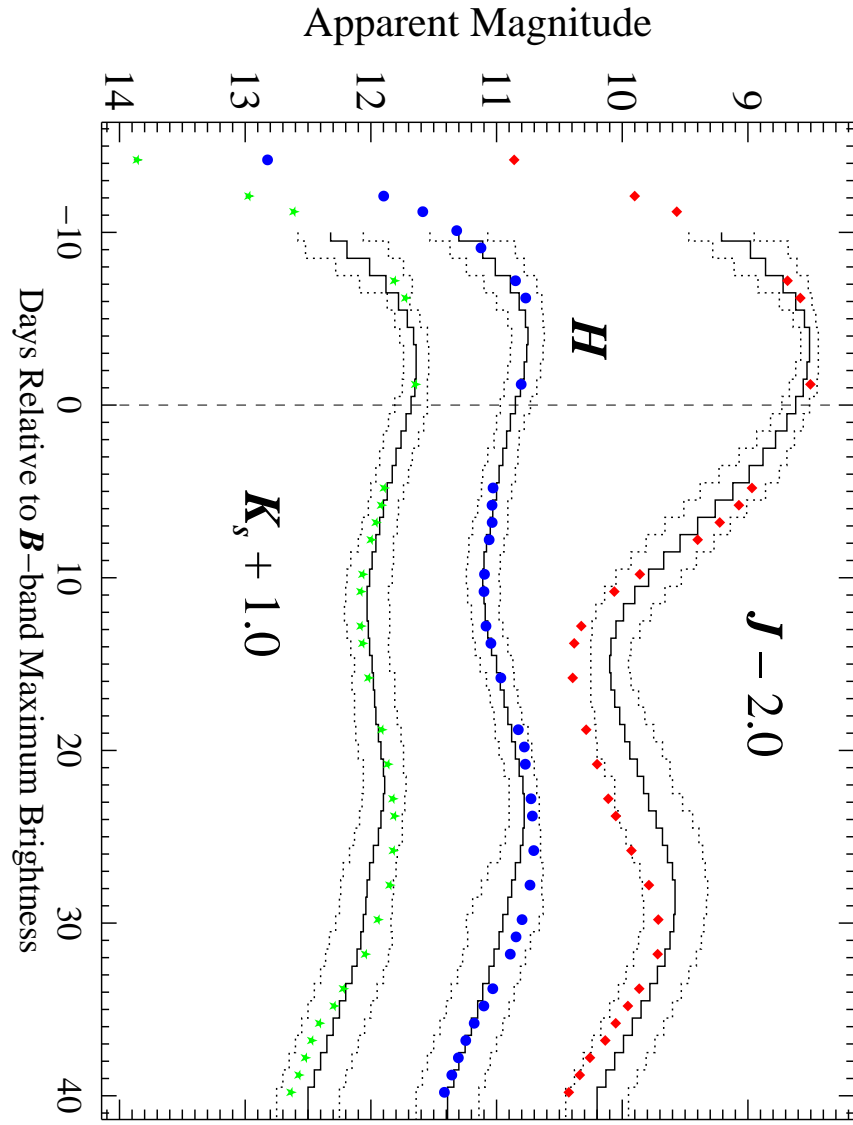


FIG. 1.— Light curves of SN 2011fe in J (red diamonds), H (blue circles), and K_s (green stars). Error bars are smaller than the plotted symbols. The J -band points are offset by -2.0 mag while the K_s -band points are offset by +1.0 mag. The templates of Wood-Vasey et al. (2008) along with their 1σ envelopes are plotted for each passband. Note that our J filter is significantly different than the 2MASS J filter used for the Wood-Vasey et al. (2008) template. The vertical dashed line marks the epoch of B -band maximum.

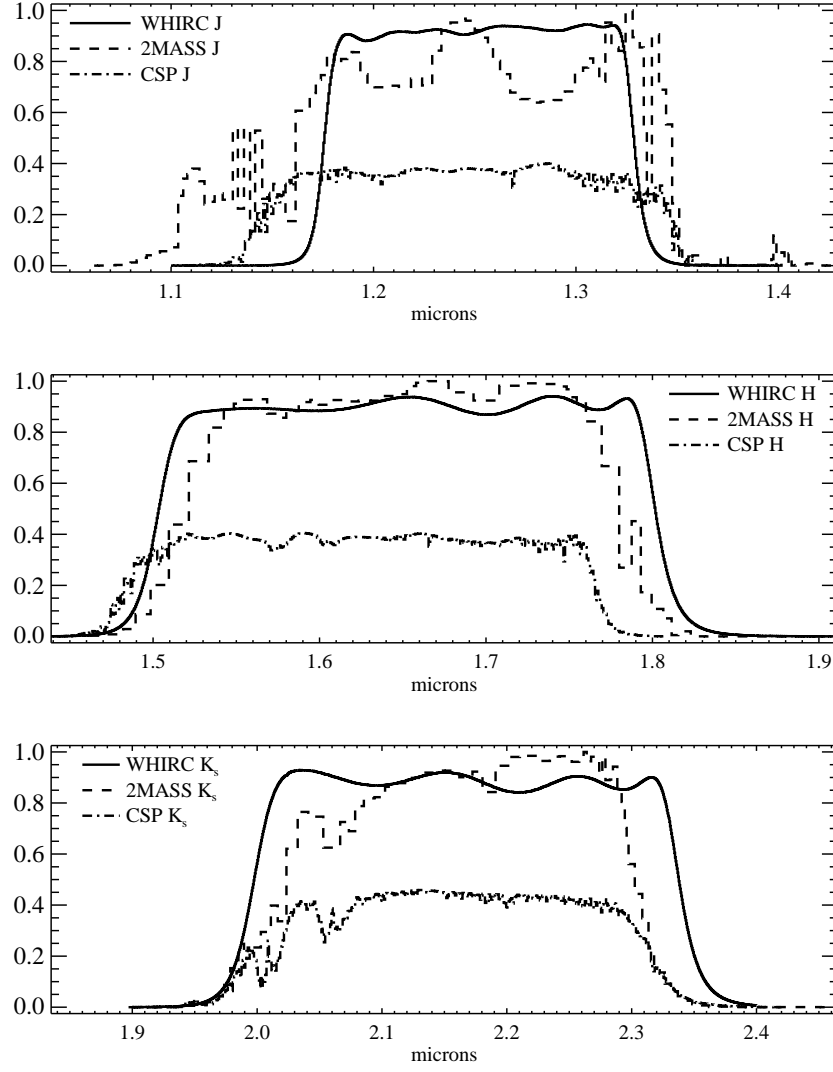


FIG. 2.— Filter bandpasses for the J , H , and K_s bands for the 2MASS filters used for the PAIRITEL data (Wood-Vasey et al. 2008), the filters used for CSP data (Contreras et al. 2010), and the WHIRC filters. For 2MASS and CSP, the bandpasses reflect the total system throughput. Only filter transmission is available for the WHIRC filters.

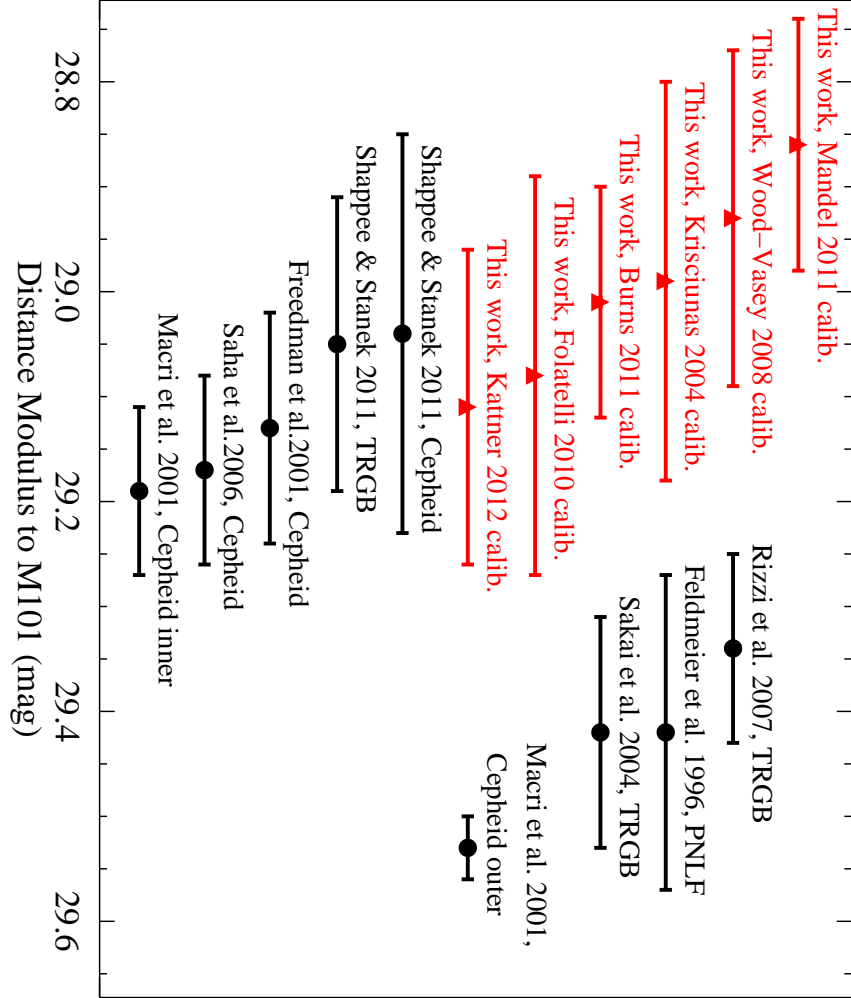


FIG. 3.— Distance moduli to M101 derived from various techniques. This is not an exhaustive list of all distances to M101, but rather a representative sample of modern values. The red triangles are distances derived from the light curve of SN 2011fe of this paper using the various calibrations of NIR SNe Ia magnitudes, all of which assume a value of $H_0 = 72 \text{ km s}^{-1} \text{ Mpc}^{-1}$. Higher values of H_0 slide the red points to the left, and lower values slide them to the right. The black squares indicate distances derived from other techniques (labeled for each point). The black points are independent of any assumed value for H_0 , and are held fixed. Error bars are 1σ .

TABLE 1
APPARENT MAGNITUDES

MJD	<i>J</i>	<i>H</i>	<i>K_s</i>
55800.121	12.860 (010)	12.822 (009)	12.855 (031)
55802.168	11.901 (010)	11.898 (008)	11.967 (029)
55803.121	11.566 (011)	11.587 (008)	11.609 (012)
55804.195	...	11.317 (010)	...
55805.199	...	11.124 (008)	...
55807.148	10.685 (013)	10.849 (008)	10.809 (014)
55808.102	10.583 (010)	10.768 (008)	10.720 (011)
55813.113	10.503 (009)	10.804 (008)	10.641 (013)
55819.133	10.968 (009)	11.028 (008)	10.890 (012)
55820.090	11.072 (009)	11.036 (008)	10.912 (011)
55821.090	11.224 (012)	11.035 (009)	10.955 (012)
55822.090	11.400 (010)	11.059 (008)	10.994 (013)
55824.090	11.860 (009)	11.096 (008)	11.061 (011)
55825.094	12.063 (009)	11.100 (008)	11.076 (012)
55827.121	12.326 (010)	11.084 (008)	11.075 (012)
55828.086	12.382 (011)	11.045 (009)	11.061 (013)
55830.109	12.394 (009)	10.966 (008)	11.014 (012)
55833.090	12.287 (011)	10.827 (008)	10.909 (012)
55834.098	...	10.779 (015)	...
55835.090	12.200 (010)	10.771 (008)	10.861 (014)
55837.086	12.111 (010)	10.726 (008)	10.821 (012)
55838.078	12.051 (010)	10.715 (008)	10.808 (013)
55840.070	11.927 (009)	10.704 (008)	10.818 (011)
55842.074	11.788 (011)	10.734 (008)	10.845 (011)
55844.074	11.713 (010)	10.797 (008)	10.939 (012)
55845.105	...	10.845 (009)	...
55846.094	11.718 (010)	10.891 (009)	11.040 (015)
55848.074	11.865 (022)	11.030 (008)	11.215 (013)
55849.070	11.955 (011)	11.101 (008)	11.289 (012)
55850.066	12.052 (009)	11.178 (010)	11.405 (026)
55851.066	12.135 (016)	11.245 (008)	11.467 (013)
55852.070	12.257 (013)	11.304 (008)	11.517 (013)
55853.062	12.338 (011)	11.356 (010)	11.569 (015)
55854.070	12.425 (012)	11.415 (010)	11.632 (013)
55860.070	12.920 (011)	11.708 (008)	11.927 (012)

TABLE 2
DERIVED DISTANCE MODULI OF M101

Calibration Source	Filter	Absolute Magnitude	Distance modulus to M101 (mag) ^a
Mandel et al. (2009) ^b	<i>J</i>	-18.25 ± 0.17	28.87 ± 0.17
	<i>H</i>	-18.01 ± 0.11	28.86 ± 0.12
	<i>K_s</i>	-18.25 ± 0.19	28.93 ± 0.20
Wood-Vasey et al. (2008) ^{b,c}	<i>J</i>	-18.29 ± 0.09	28.91 ± 0.10
	<i>H</i>	-18.08 ± 0.15	28.93 ± 0.16
	<i>K_s</i>	-18.32 ± 0.26	29.00 ± 0.26
Krisciunas et al. (2004a) ^d	<i>J</i>	-18.57 ± 0.14	29.08 ± 0.14
	<i>H</i>	-18.24 ± 0.18	28.99 ± 0.19
	<i>K_s</i>	-18.42 ± 0.12	29.06 ± 0.13
Folatelli et al. (2010) ^b	<i>J</i>	-18.42 ± 0.18	29.04 ± 0.18
	<i>H</i>	-18.23 ± 0.19	29.08 ± 0.19
	<i>K_s</i>	-18.30 ± 0.27	28.98 ± 0.27
Folatelli et al. (2010) ^d	<i>J</i>	-18.43 ± 0.18	28.94 ± 0.18
	<i>H</i>	-18.42 ± 0.19	29.17 ± 0.19
	<i>K_s</i>	-18.47 ± 0.27	29.11 ± 0.27
Burns et al. (2011) ^d	<i>J</i>	-18.44 ± 0.12	28.94 ± 0.13
	<i>H</i>	-18.26 ± 0.10	29.01 ± 0.11
Kattner et al. (2012) ^{d,e}	<i>J</i>	-18.57 ± 0.14	29.08 ± 0.15
	<i>H</i>	-18.42 ± 0.14	29.17 ± 0.15

^a Distance modulus calculated by combining absolute magnitude with the apparent magnitudes for SN 2001fe derived from our light curves (see text for details). This is conditional on $H_0 = 72 \text{ km s}^{-1} \text{ Mpc}^{-1}$.

^b Fiducial time is *B*-band maximum brightness.

^c Using PAIRTEL subsample only.

^d Fiducial time is maximum brightness in the given filter (*J*, *H*, or *K_s*).

^e Using subsample 2 of Kattner et al. (2012).